Journal of Solid State Chemistry **163,** 224–230 (2002)
doi:10.1006/jssc.2001.9396, available online at http://www.idealibrary.com on IDEAL®

Time-Dependent Degradation Due to the Gradual Phase Change in BICUVOX and BICOVOX Oxide-Ion Conductors at Temperatures below about 500°C

Akiteru Watanabe and Kaushik Das

Advanced Materials Laboratory, National Institute for Materials Science, 1-1 Namiki, Tsukuba, Ibaraki 305-0044, Japan

Recieved April 4, 2001; in revised form September 5, 2001; accepted September 14, 2001

This paper describes a cause of the time-dependent degradation of conductivity observed in the representative BIMEVOX phases $Bi_2Cu_{0.1}V_{0.9}O_{5.35}$ (BICUVOX.10) and $Bi_2Co_{0.1}V_{0.9}O_{5.35}$ (BICOVOX.10). In both phases, to date, the following facts were reported: the high-temperature stable γ-type phase transformed reversibly to the low-temperature stable γ'-type phase at 450–500°C through the order–disorder transition without changing to the β-type or α-type phase. In addition, the degradation of conductivity was observed in γ'-BICUVOX.10 at about 420°C. In the present study, it has turned out that a prolonged annealing at 450°C for several hundred hours causes both γ' phases to change to a new phase with α-$Bi_4V_2O_{11}$-related structure. This α-related phase changes promptly to the γ phase on heating (at about 535°C for BICOVOX.10 and at about 485°C for BICUVOX.10); by contrast, the γ' phase reverts sluggishly to the α-related phase. Since the α-related phase shows far lower conductivity ($10^{-4.8}$ S cm^{-1} at 430°C for BICUVOX.10), this gradual γ'-to-α transition explains well the time-dependent degradation of conductivity in the γ' phase reported so far. Namely, the γ' phase is metastably quenched to room temperature and reverts gradually to the α-related phase upon heat treatment below the α-to-γ transition temperature. © 2002 Elsevier Science

Key Words: **$Bi_2Cu_{0.1}V_{0.9}O_{5.35}$ (BICUVOX.10); $Bi_2Co_{0.1}V_{0.9}O_{5.35}$ (BICOVOX.10); prolonged annealing; α-$Bi_4V_2O_{11}$-related phase; gradual γ'-to-α transition; degradation of conductivity.**

INTRODUCTION

The BIMEVOX group given by the formula $Bi_2V_{1-x}Me_xO_{5.5-\delta}$ (1) is derived from the partial substitution of various metal atom, *Me*, for vanadium in the parent oxide $Bi_4V_2O_{11}$ (2–4). The compound $Bi_4V_2O_{11}$ possesses three polymorphs labeled α, β, and γ: the α form is the low-temperature stable modification, the β form the intermediate one, and the γ form the high-temperature stable one which shows a high oxide-ion conduction (4). Thus, depending on *Me* and x in $Bi_2V_{1-x}Me_xO_{5.5-\delta}$, the prepared BIMEVOX solid solution had an isomorphous structure or a very closely related structure with one of three modifications at room temperature. For instance, in both cases of Me = Mo(VI) (5) and W(VI) (6), α-type BIMEVOX ($0 \le x < 0.05$) and β-type BIMEVOX ($0.05 \le x \le 0.125$) solid solutions existed stably, but γ-type BIMEVOX did not exist stably. On the other hand, in Me = Cu(II) (7, 8), stable α-type ($0 \le x \le 0.06$) and γ-type ($0.075 \le x \le 0.15$) BIMEVOX solid solutions were identified. Many elements such as Mg(II), Co(II), Zn(II), Fe(III), etc. (9–15), were also possible to substitute for vanadium to bring a stable γ-type BIMEVOX solid solution within a limited compositional region in the same manner as Cu; in addition, the best oxide-ion conductivity characteristics were always obtained in the γ-type BIMEVOX solid solution with an x value close to 0.10 independent of *Me* (10), e.g., 1×10^{-3} S cm^{-1} around 240°C for $Bi_2Cu_{0.1}V_{0.9}O_{5.35}$ (1). To be brief, for various metal atom *Me*, the BIMEVOX with $x = 0.10$ can possess only the γ-type structure stably at lower temperatures and exhibit a very high oxide-ion conduction.

For this reason, many researchers directed their attention to representative compositions of $Bi_2Cu_{0.1}V_{0.9}O_{5.35}$ (BICUVOX.10) (7, 16–22) and $Bi_2Co_{0.1}V_{0.9}O_{5.35}$ (BICOVOX.10) (23–26). At the same time, a polymorphic transformation was found in both phases at 450–500°C (7, 18–23, 26). Thereafter, the high-temperature BIMEVOX phase was called γ-BIMEVOX and the low-temperature one termed γ'-BIMEVOX. The subsequent study indicated that γ'-BIMEVOX has a complex incommensurate superstructure (7). Thus this transformation is considered to be attributable to the partial ordering of oxide ions. Despite the ordering, γ'-BIMEVOX exhibits a relatively high conductivity. On one hand, a prolonged annealing of γ'-BICUVOX at 424°C brought about considerable degradation in conductivity (22). However, very little is known about the origins of this degradation.

The purpose of this paper is to elucidate a factor of the degradation from the point of view of phase equilibrium. As

0022-4596/02 $35.00

a result, a new phase is found by prolonged annealing at 450°C in both BICUVOX.10 and BICOVOX.10; the new phase has an α-$Bi_4V_2O_{11}$-related structure and yields too low conductivity to apply themselves to electrochemical devices.

EXPERIMENTAL PROCEDURE

The starting materials were 99.9% pure Bi_2O_3, V_2O_5, CuO, and CoO. The γ′-BICUVOX.10 and γ′-BICOVOX.10 were synthesized from the stoichiometric mixture by solid-state reaction in air at 800°C for 20 h. Subsequently, to check the time-dependent character, part of each γ′-BIMEVOX.10 was annealed at 450°C for 450 h or more, and the same heat treatment was repeated several times with intermediate quenching and grinding in order to ensure the completion of reaction. At the end of each reaction, the product was quenched by an air stream to room temperature. All products were examined by XRPD using Cu$K\alpha$ radiation and a diffracted-beam monochromator.

Thermal behavior was checked by differential thermal analysis (DTA) using Rigaku TG-8120 apparatus. About 50 mg of the sample put in a platinum sample holder underwent heating–cooling cycles in air at a rate of 5°C min^{-1} to the maximum temperature of 625°C. The reference material was α-Al_2O_3, and the temperature accuracy was $\pm$ 3°C.

Electrical conductivity was measured by means of the impedance spectroscopy method in air on pellets fabricated by the following procedure. Powder sample was thoroughly ground in an agate mortar and checked with SEM for their grain size distribution. Modal concentration shows that nearly 80% of the grains are smaller than 5 μm and 20% of the grains are in the size range 10 to 15 μm. Such powder was prepressed uniaxially (10 mm in diameter and 1.6–2.3 mm thick) and then pressed isostatically at 200 MPa. The pellets were sintered at 800°C for 20 h in γ′-BIMEVOX.10 and at 450°C for 470 h in the low-temperature phases. Then both flat surfaces of the pellets were smeared with platinum paste as electrodes. All the pellets were studied by Solartron SI-1260 impedance analyzer in the frequency range 1 Hz to 1 MHz at every 20°C interval between 150 and 710°C through heating–cooling cycles. The sample pellets were equilibrated at constant temperature for 20 min before each measurement. Bulk conductivity values were obtained from complex impedance plots and represented in the form of Arrhenius plot, i.e., $\log[\sigma\,(S\,cm^{-1})] - 1/T\,(K^{-1})$.

RESULTS AND DISCUSSION

Figures 1a and 2a show the powder XRPD patterns of γ′-BICOVOX.10 and γ′-BICUVOX.10 equilibrated at 800°C, respectively. Both patterns agree well with those reported: $a = 3.907$ Å and $c = 15.41$ Å for γ′-BICUVOX (1)

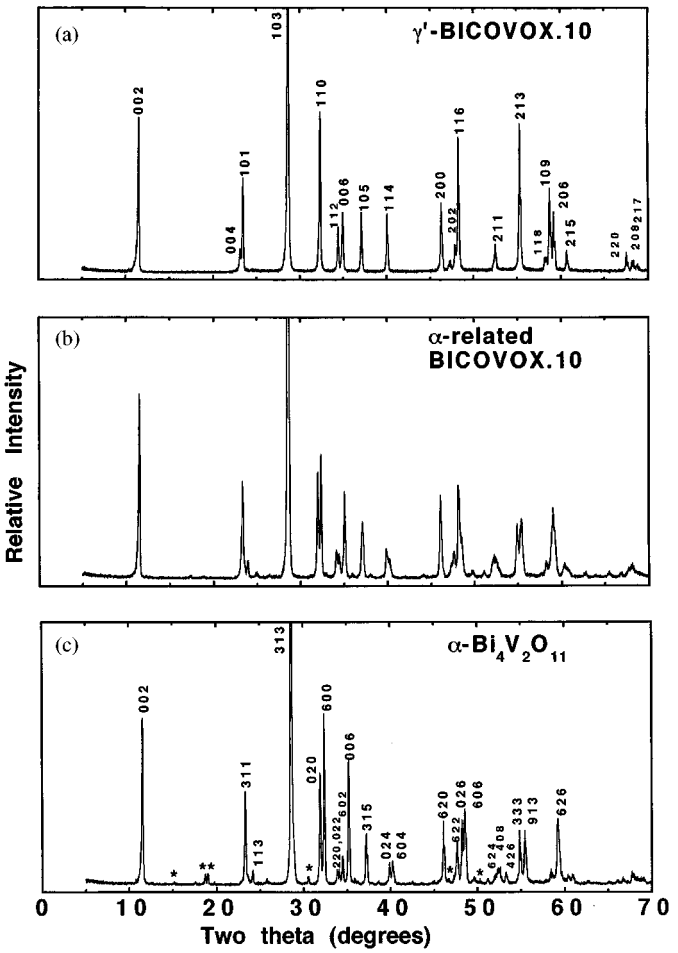

FIG. 1. XRPD patterns for BICOVOX.10: (a) γ′ phase equilibrated at 800°C, (b) α-related phase equilibrated at 450°C, and (c) α-$Bi_4V_2O_{11}$ prepared at 800°C, where asterisked reflections are caused by $BiVO_4$.

and $a = 3.927$ Å and $c = 15.42$ Å for γ′-BICOVOX.10 (27). On the other hand, the samples equilibrated at 450°C show quite obvious changes in the XRPD patterns (Figs. 1b and 2b); as a whole, both patterns resemble to that of α-$Bi_4V_2O_{11}$, which is the low-temperature stable modification crystallizing in the orthorhombic symmetry with $a = 16.559$ Å, $b = 5.611$ Å, and $c = 15.288$ Å (4), as shown in Fig. 1c where asterisked reflections are from $BiVO_4$ which is inevitably generated as another phase in a two-phase region of the system Bi_2O_3–V_2O_5 (28). Hereafter, therefore, the new phases corresponding to Figs. 1b and 2b are designated the α-related phase for convenience. To date, since it is firmly believed that BICUVOX.10 and BICOVOX.10 exist stably as the γ′-type phase at lower temperatures than 450–500°C, no one has detected the present phase change as well as the α-related phase. However, we could not index both α-related XRPD patterns because of the broad peaks. The doublet of the strongest peak pointed out in the inlet

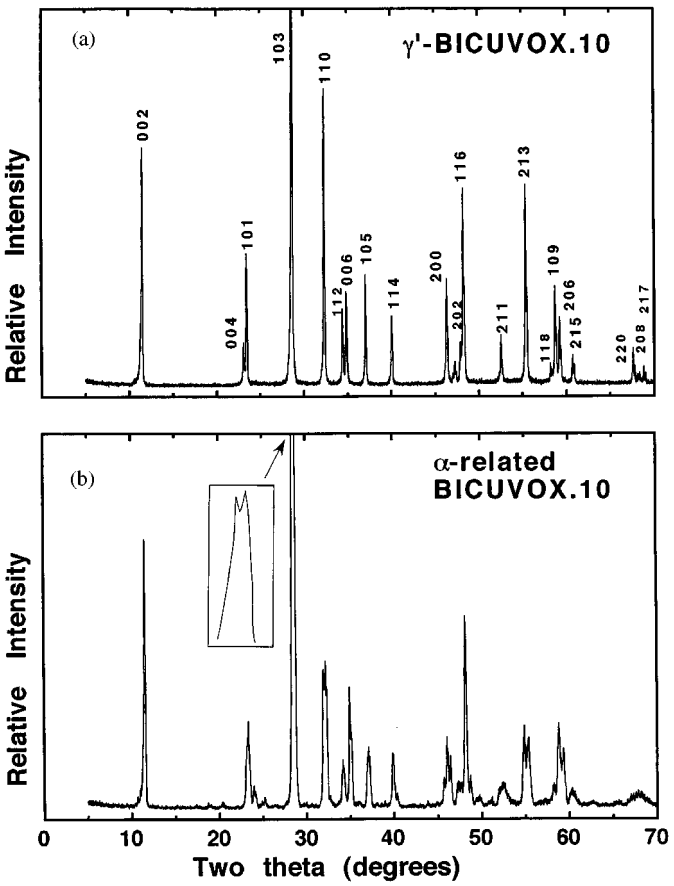

FIG. 2. XRPD patterns for BICUVOX.10: (a) γ' phase equilibrated at 800°C, and (b) α-related phase equilibrated at 450°C. (Inset) Magnified peak detail of the strongest reflection.

of Fig. 2b implies that the α-related phase might have a monoclinic structure in the same manner as reported by Joubert *et al.* (29) in α-$Bi_4V_2O_{11}$. The formation of the α-related phase denotes the metastability of the γ' phase.

Figure 3a shows DTA results of γ'-BICOVOX.10 equilibrated at 800°C. A small endothermic peak appears at about 500°C on heating and a small exothermic peak is observed at about 480°C on cooling. The second cycle reproduces the same results without thermal hysteresis. This reversible thermal effect indicates a γ'-to-γ transition. On one hand, as shown in Fig. 3b, α-related BICOVOX.10 equilibrated at 450°C undergoes a clear endothermic peak at 535°C in the first heating direction; this thermal effect is caused by the α-to-γ transition. The considerable structural difference between the α-related phase and the γ-phase may lead to the somewhat large transformation enthalpy change. On subsequent cooling, however, the DTA trace shows a diffuse exothermic peak at about 470°C. This peak indicates the γ-to-γ' transition which corresponds to the exothermic peak at 480°C in Fig. 3a. By contrast, in the second heating cycle, an only perceptible inflection corresponding to the γ'-to-γ transition is observed at about 460°C. Although the α-related phase changes easily at 535°C to the γ phase on heating, the γ phase never revert to the α-related phase on cooling under the present DTA conditions, because the γ-to-α transition proceeds far sluggishly compared to the reverse α-to-γ transition. The γ phase preferentially transforms to the metastable γ' phase on account of the close structural relation between the γ and γ' phases as mentioned in the Introduction. In $Bi_5Pb_3O_{10.5}$ (30, 31), we could observe the same thermal behavior as BIMEVOX; namely, the high-temperature stable β form transforms inevitably to the metastable β_2 form on cooling because of the structural similarity between two forms despite the existence of the low-temperature stable β_L form. Thus, now that γ'-BICOVOX.10 is metastable below 535°C, it is necessary for the pure α-related phase preparation to anneal the γ' phase at temperatures below 535°C for a somewhat long time, e.g., at 450°C for 450 h or more as described under Experimental procedure. Likewise, in BICUVOX.10, we can observe DTA results similar to those of BICOVOX.10. Figure 3c shows a reversible γ'-to-γ transition at 480°C as reported by Pernot *et al.* (7) and Simner *et al.* (23). Figure 3d represents that the α-related phase changes at 485°C to the γ phase.

It is evident from the above results (Figs. 1, 2, and 3) that γ'-BICOVOX.10 and γ'-BICUVOX.10 revert finally to the α-related phase by annealing at temperatures below the α-to-γ transition (535°C for BICOVOX.10 and 485°C for BICUVOX.10) for several hundred hours. In addition, since a rate of the γ'-to-α transition is notably sluggish, the γ' phases are readily quenched to room temperature. It seems that the α-related phase is the low-temperature stable form.

Figure 4a shows Arrhenius plots of electrical conductivity for γ'-BICUVOX.10 equilibrated at 800°C. The pellet underwent the heating–cooling cycle four times. Since all cooling-cycle conductivity values were the same as those of the third heating cycle (designated by the open circles in Fig. 4a), only the heating-cycle data are plotted. All curves show the γ'-to-γ transition over 450–490°C ($10^4/T$ = 13.1–13.8 K^{-1}), and the conductivity values of the γ phase are almost the same for all the cycles. It is noted, however, that the conductivity values of the γ' phase show not only the thermal hysteresis except the third cycle but also the disparity except the second and the fourth cycles. The disparity depends on the period for which the pellet was left at room temperature before each cycle. That is, the pristine pellet was kept for a few days in a desiccator at room temperature prior to the first measurement; before the second cycle, the pellet was left for one night at room temperature in a furnace on the apparatus. By contrast, the third cycle was carried out subsequently just after the second one. There was the same interruption between the third and the fourth cycles as that between the first and the second cycles.

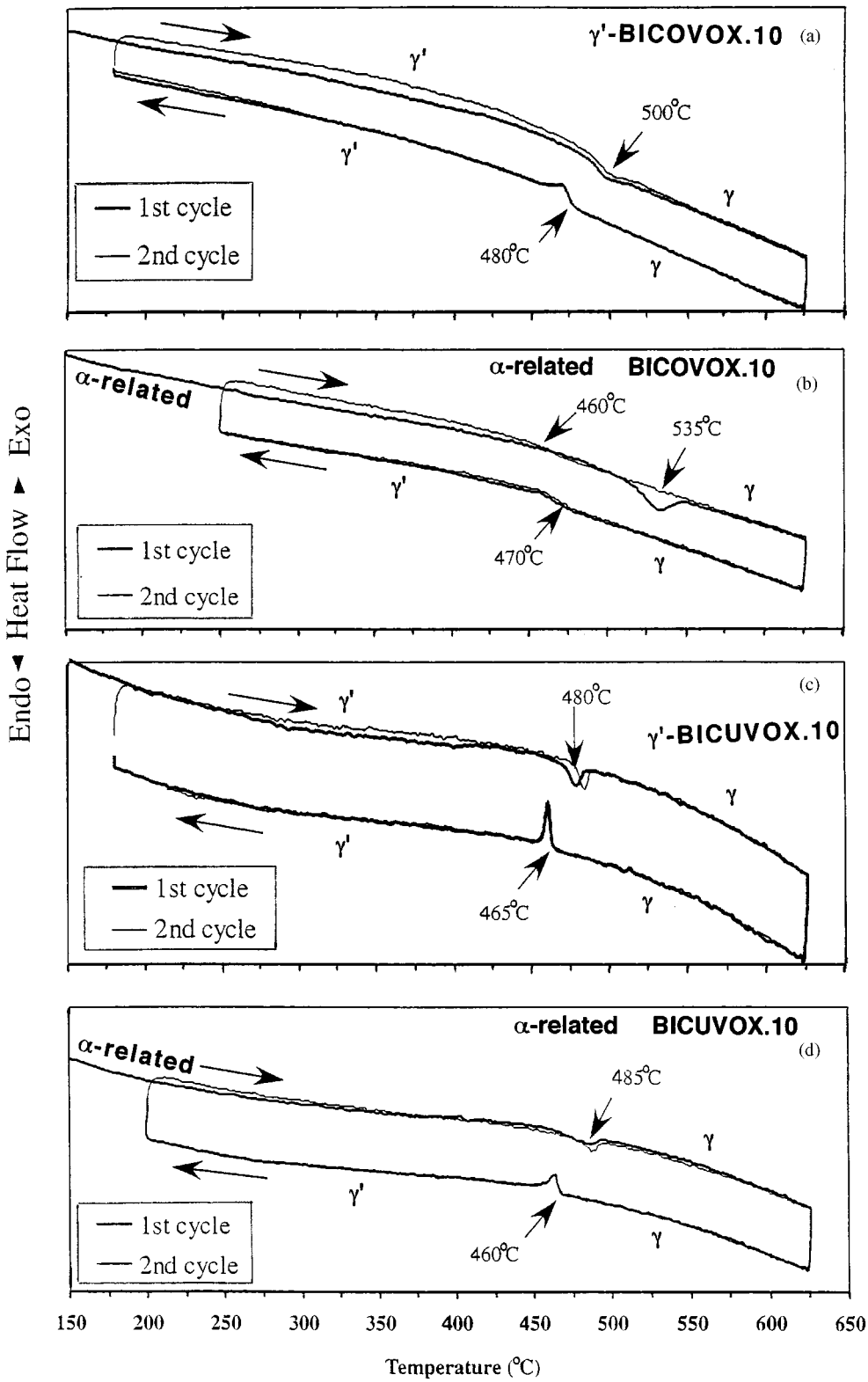

FIG 3. DTA curves for the starting materials of (a) γ'-BICOVOX.10 equilibrated at 800°C, (b) α-related BICOVOX.10 equilibrated at 450°C, (c) γ'-BICUVOX.10 equilibrated at 800°C, and (d) α-related BICUVOX.10 equilibrated at 450°C.

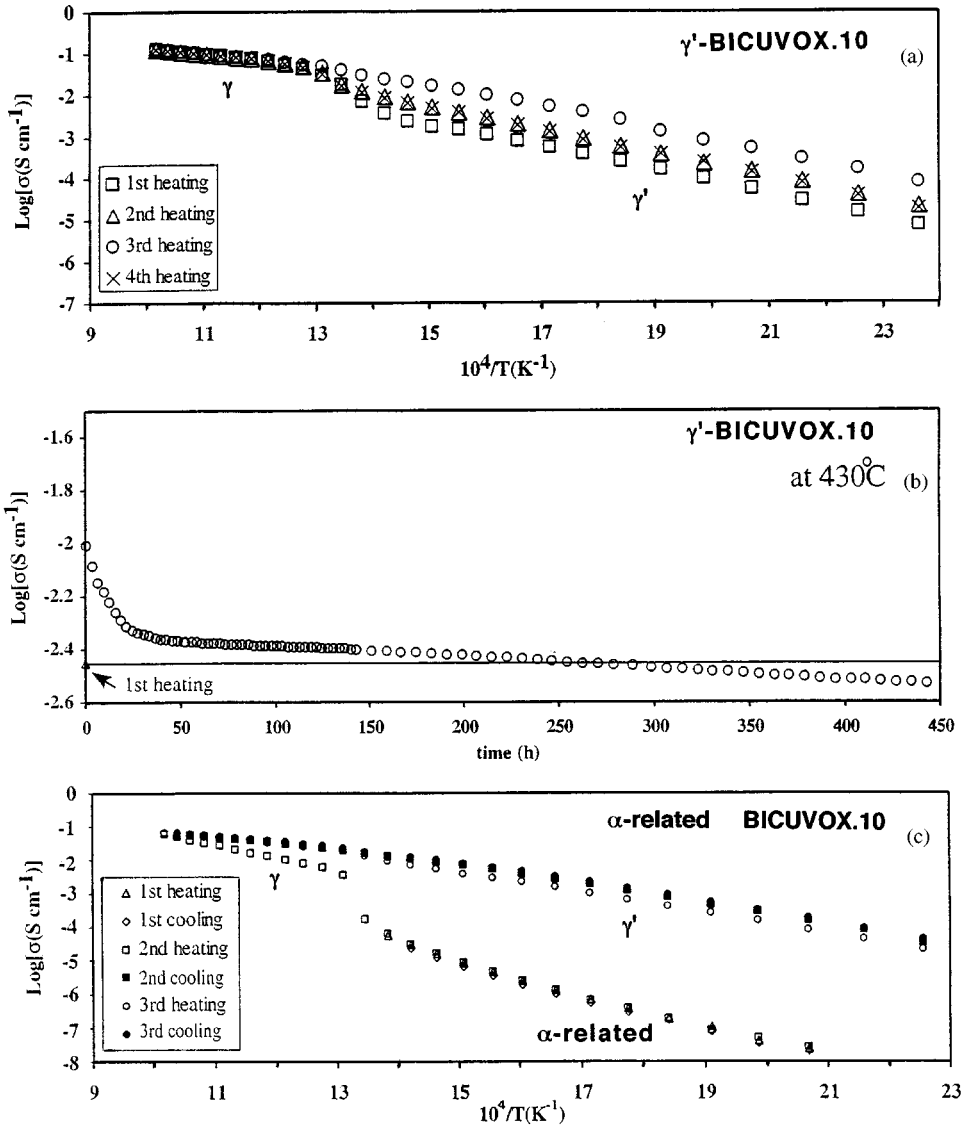

FIG. 4. Variations of electrical conductivity for BICUVOX.10 with temperature and with time: (a) Arrhenius plots of the starting γ' phase equilibrated at 800°C, (b) time-dependent degradation at 430°C of the same sample as (a) which underwent four times heating–cooling cycle, and (c) Arrhenius plots of the starting α-related phase equilibrated at 450°C. The horizontal line depicted in (b) denotes $\log\sigma = -2.45$ equivalent to that of the first heating in (a) at 430°C.

Thus, the γ' phase exhibits a "time-dependent aging" phenomenon. In other words, the metastability of the γ' phase seems to bring about the gradual transition to the α-related phase even at room temperature.

In order to examine the aging phenomenon, the electrical conductivity measurement was subsequently conducted on the same pellet as above at a constant temperature of 430°C ($10^4/T = 14.2\ \mathrm{K}^{-1}$) below the γ'-to-γ transition point of 480°C (Fig. 3c). The variation of conductivity with time is shown in Fig. 4b. The initial conductivity of $\log\sigma = -2$ drops to -2.3 after 24 h, and then decreases somewhat slowly to a value lower than -2.45 after 300 h; as indicated in a horizontal line inset in Fig. 4b, the $\log\sigma = -2.45$ corresponds to the conductivity at 430°C of the pristine pellet under the first heating cycle shown in Fig. 4a. Namely, this result implies that the heat treatment at 430°C causes the γ' phase to transform into the α-related phase.

Figure 4c represents Arrhenius plots of electrical conductivity for α-related BICUVOX.10 equilibrated at 450°C. In the first heating–cooling cycle measured up to 450°C ($10^4/T = 13.8\ \mathrm{K}^{-1}$), very low conductivity values are observed without hysteresis. In the subsequent second heating direction, the values coincide with those of the first cycle until 450°C, and then indicate the α-to-γ transition clearly at

470–490°C. On the second cooling, we can observe not only the perceptible γ-to-γ' transition around 470°C but also the noticeable hysteresis in the γ phase region. The hysteresis seems to be attributable to the poor sintering of the pellet which was sintered at 450°C; however, the pellet underwent the maximum temperature of 710°C, so that the sintering proceeded largely to yield higher conductivity of the γ phase on cooling.

Although Fig. 4b demonstrates the time-dependent degradation of the γ' phase up to 450 h, we can estimate from Fig. 4c the final conductivity value annealed at 430°C for infinite time. That is, as a result of degradation, the metastable γ' phase changes completely to the α-related phase, so that the conductivity value of 430°C plotted in Fig. 4c corresponds to the final value, $\log\sigma = -4.8$.

As for γ'-BICUVOX.10, Dygas *et al.* (22) also reported the thermal hysteresis of conductivity depending on heat treatments; their results are similar to our results (Fig. 4a). At the same time, they described the time-dependent conductivity degradation of which a rate is faster than our results (Fig. 4b). In fact, the composition of their sample was not $Bi_2Cu_{0.1}V_{0.9}O_{5.35}$ but $Bi_2Cu_{0.06}V_{0.84}O_{5.16}$ (20). According to our recent preliminary experiment, the γ'-$Bi_2Cu_{0.06}V_{0.84}O_{5.16}$ changed relatively rapidly by annealing at 450°C to a product which showed a more complex XRPD pattern than that of the α-related phase (Fig. 2b).

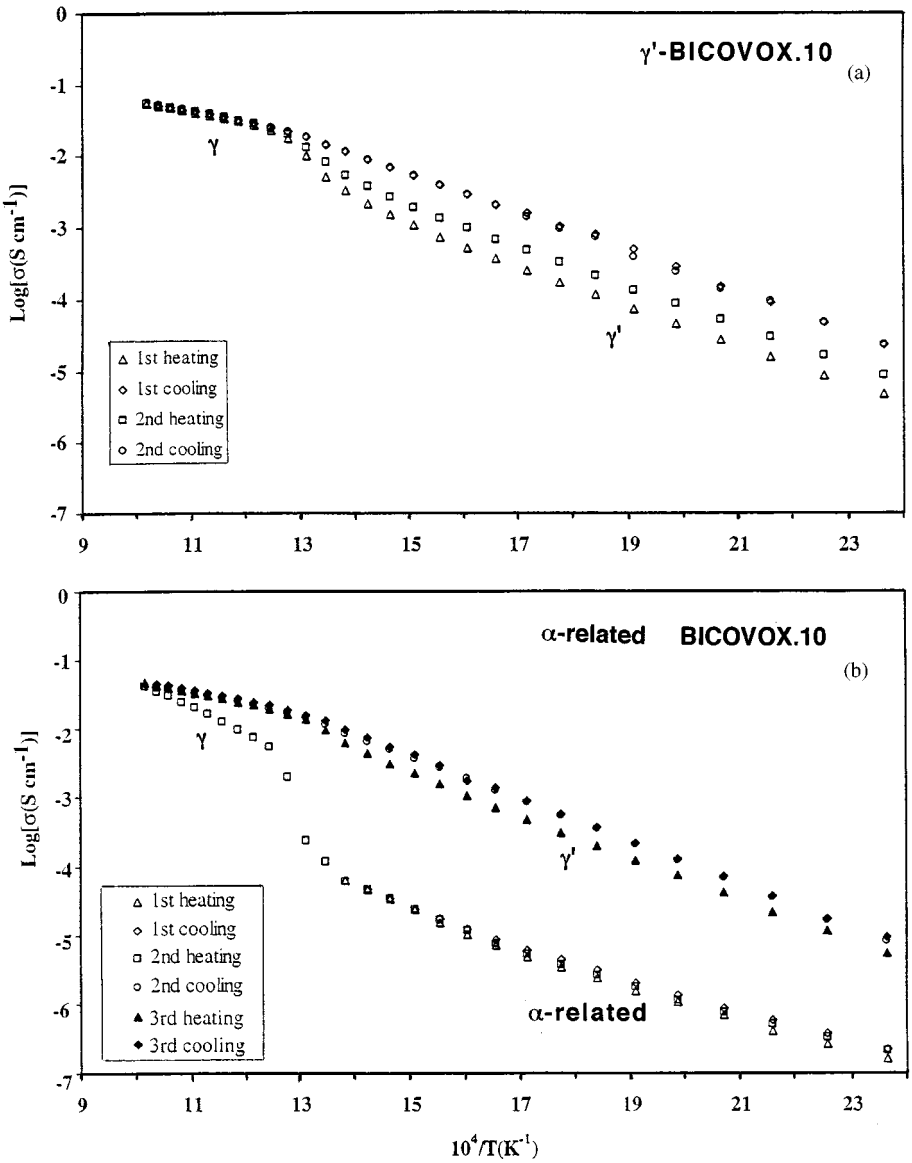

FIG. 5. Arrhenius plots of electrical conductivity of BICOVOX.10 for the starting phases of (a) γ' phase equilibrated at 800°C and (b) α-related phase equilibrated at 450°C.

Therefore, the reason for the rate difference lies in the compositional difference between theirs and ours. Although they concluded that the thermal hysteresis of conductivity was ascribed to the microstructure such as a grain size and that the degradation was caused by a slow ordering process within the perovskite-like $V_{0.9}Cu_{0.1}O_{3.35}$ sheets, both thermal hysteresis and degradation are attributed to the sluggish γ'-to-α transformation as mentioned above.

In the case of BICOVOX.10, Arrhenius plots of conductivity can be explained in the same way as BICUVOX.10. Figure 5a shows the time-dependent thermal hysteresis of the γ' phase equilibrated at 800°C: the pristine pellet was kept for a few days at room temperature prior to the first measurement, and after the first cycle, the pellet was left for one night at room temperature in the furnace on the apparatus. Figure 5b represents that the α-to-γ transition occurs over a temperature range of 470–530°C in contrast to 535°C by DTA (Fig. 3b). The third heating cycle gives the γ'-to-γ transition over a temperature range of 470–490°C with relation to 500°C by DTA (Fig. 3a). Steil *et al.* (26) described the same behavior of conductivity as Fig. 5a. However, they also ascribed this phenomenon to the grain size, because they found neither the α-related phase nor the γ'-to-α transformation. The existence of the α-related phase means that the time-dependent degradation is observed below 535°C in BICOVOX.10 also. Thus, as can be seen from Figs. 4 and 5, the time-dependent aging phenomenon is ascribable to the phase transition from the metastable γ' phase to the stable α-related phase. Moreover, the metastability of the γ' phase seems to bring about the gradual transition to the α-related phase even at room temperature.

CONCLUSION

The solid electrolyte conductivity should be stable against prolonged heat treatments for an application of it to electrochemical devices. To date, although BICUVOX and BICOVOX have been considered a very promising material, the present study elucidates the metastability of these phases. That is, γ'-BICUVOX.10 and γ'-BICOVOX.10 transforms very sluggishly to the new phase, which shows far lower conductivity, below about 485°C and about 535°C, respectively. As a result, when these γ' phases are treated at temperatures below their transition temperatures, the time-dependent degradation in conductivity is observed and the conductivity is finally depressed to some level far from usefulness. To avoid the degradation, we have to suppress the formation of the α-related phase by means of the grain size control, the further addition of other material(s), etc. Probably, only the high-temperature stable γ phase can be applicable to some devices above their transition temperatures. The thermal stability of other members of BIMEVOX group and the true stabilization of the γ phase will be the subject of future studies.

ACKNOWLEDGMENT

This study was supported by CREST of Japan Science and Technology.

REFERENCES

1. F. Abraham, J. C. Boivin, G. Mairesse, and G. Nowogrocki, *Solid State Ionics* **40/41,** 934 (1990).
2. A. A. Bush and Yu. N. Venevtsev, *Russ. J. Inorg. Chem.* **31,** 769 (1986).
3. Ya. N. Blinovskov and A. A. Fotiev, *Russ. J. Inorg. Chem.* **32,** 145 (1987).
4. F. Abraham, M. F. Debreuille-Gresse, G. Mairesse, and G. Nowogrocki, *Solid State Ionics* **28–30,** 529 (1988).
5. R. N. Vannier, G. Mairesse, F. Abraham, and G. Nowogrocki, *J. Solid State Chem.* **103,** 441 (1993).
6. R. N. Vannier, G. Mairesse, F. Abraham, and G. Nowogrocki, *Solid State Ionics* **80,** 11 (1995).
7. E. Pernot, M. Anne, M. Bacmann, P. Strobel, J. Fouletier, R. N. Vannier, G. Mairesse, F. Abraham, and G. Nowogrocki, *Solid State Ionics* **70/71,** 259 (1994).
8. C. K. Lee, G. S. Lim, and A. R. West, *J. Mater. Chem.* **4,** 1441 (1994).
9. R. N. Vannier, G. Mairesse, G. Nowogrocki, F. Abraham, and J. C. Boivin, *Solid State Ionics* **53–56,** 713 (1992).
10. G. Mairesse, in "Fast Ion Transport in Solids" (B. Scrosati, A. Magishis, C. M. Mari, and G. Mariotto, Eds.), p. 271. Kluwer, Dordrecht, 1993.
11. C. K. Lee, M. P. Tan, and A. R. West, *J. Mater. Chem.* **4,** 525 (1994).
12. O. Joubert, A. Jouanneaux, M. Ganne, R. N. Vannier, and G. Mairesse, *Solid State Ionics* **73,** 309 (1994).
13. S. Lazure, R. N. Vannier, G. Nowogrocki, G. Mairesse, C. Muller, M. Anne, and P. Strobel, *J. Mater. Chem.* **5,** 1395 (1995).
14. O. Joubert, M. Ganne, R. N. Vannier, and G. Mairesse, *Solid State Ionics* **83,** 199 (1996).
15. J. C. Boivin, C. Pirovano, G. Nowogrocki, G. Mairesse, Ph. Labrune, and G. Lagrange, *Solid State Ionics* **113–115,** 639 (1998).
16. F. Krok, I. Abrahams, M. Malys, W. Bogusz, J. R. Dygas, J. A. G. Nelstrop, and A. J. Bush, *Solid State Ionics* **136–137,** 119 (2000).
17. T. Iharada, A. Hammouche, J. Fouletier, M. Kleitz, J. C. Boivin, and G. Mairesse, *Solid State Ionics* **48,** 257 (1991).
18. F. Krok, W. Bogusz, P. Kurek, M. Wasiucionek, W. Jakubowski, and J. Dygas, *Mater. Sci. Eng.* **B21,** 70 (1993).
19. K. Reiselhuber, G. Dorner, and M. W. Breiter, *Electrochim. Acta* **38,** 969 (1993).
20. P. Kurek, J. R. Dygas, and M. W. Breiter, *J. Electroanal. Chem.* **378,** 77 (1994).
21. J. R. Dygas, F. Krok, W. Bogusz, P. Kurek, K. Reiselhuber, and M. W. Breiter, *Solid State Ionics* **70/71,** 239 (1994).
22. J. R. Dygas, P. Kurek, and M. W. Breiter, *Electrochim. Acta* **40,** 1545 (1995).
23. S. P. Simner, D. Suarez-Sandoval, J. D. Mackenzie, and B. Dunn, *J. Am. Ceram. Soc.* **80,** 2563 (1997).
24. F. Krok, I. Abrahams, D. G. Bangobango, W. Bogusz, and J. A. G. Nelstrop, *Solid State Ionics* **86–88,** 261 (1996).
25. S.-K. Kim and M. Miyayama, *Solid State Ionics* **104,** 295 (1997).
26. M. C. Steil, J. Fouletier, M. Kleitz, and P. Labrune, *J. Eur. Ceram. Soc.* **19,** 815 (1999).
27. Powder Diffraction File 86–104. International Center for Diffraction Data, Swathmore, PA.
28. A. Watanabe, *J. Solid State Chem.* **161,** 410 (2001).
29. O. Joubert, A. Jouanneaux, and M. Ganne, *Mater. Res. Bull.* **29,** 175 (1994).
30. A. Watanabe, Y. Kitami, S. Takenouchi, J. C. Boivin, and N. Sammes, *J. Solid State Chem.* **144,** 195 (1999).
31. A. Watanabe, *Solid State Ionics* **136,** 115 (2000).